arXiv:astro-ph/0010427v1 20 Oct 2000

AN IMAGING AND SPECTROSCOPIC STUDY OF THE $z_{\rm abs} = 3.38639$ DAMPED Lyα SYSTEM IN Q0201+1120: CLUES TO STAR FORMATION AT HIGH REDSHIFT [1]

Sara L. Ellison
Institute of Astronomy, Madingley Road, Cambridge, CB3 0HA, UK and
European Southern Observatory, Casilla 19001, Santiago 19, Chile

Max Pettini
Institute of Astronomy, Madingley Road, Cambridge, CB3 0HA, UK

Charles C. Steidel[2] and Alice E. Shapley
Palomar Observatory, Caltech 105–24, Pasadena, CA 91125

[1]Based in large part on observations obtained at the W.M. Keck Observatory, which is operated as a scientific partnership among the California Institute of Technology, the University of California, and NASA, and was made possible by the generous financial support of the W.M. Keck Foundation.

[2]Packard Fellow

ABSTRACT

We present the results of a series of imaging and spectroscopic observations aimed at identifying and studying the galaxy responsible for the $z_{\rm abs} = 3.38639$ damped Lyman α system in the $z_{\rm em} = 3.61$ QSO Q0201+1120. We find that the DLA is part of a concentration of matter which includes at least four galaxies (probably many more) over linear comoving dimensions greater than $5h^{-1}$ Mpc. The absorber may be a $0.7L^*$ galaxy at an impact parameter of $15h^{-1}$ kpc, but follow-up spectroscopy is still required for positive identification. The gas is turbulent, with many absorption components distributed over ~ 270 km s^{-1} and a large spin temperature, $T_s \gtrsim 4000$ K. The metallicity is relatively high for this redshift, $Z_{\rm DLA} \simeq 1/20 Z_\odot$. From consideration of the relative ratios of elements which have different nucleosynthetic timescales, it would appear that the last major episode of star formation in this DLA occurred at $z \gtrsim 4.3$, more than ~ 500 Myr prior to the time when we observe it.

Subject headings: cosmology:observations — galaxies:abundances — galaxies:evolution — quasars:absorption lines – quasars: individuals (Q0201+1120)

1. INTRODUCTION

The study of quasar absorption lines is a unique tool with which to investigate the high redshift universe on a variety of scales, ranging from the intergalactic medium (IGM) to proto-galaxies. Since the detection of material intercepting our line of sight to a given QSO is dependent only on the column density of gas and the luminosity of the quasar, this is a particularly powerful and sensitive technique for probing the chemical composition and physical conditions in the interstellar media (ISM) of high z galaxies.

Damped Lyman Alpha systems (DLAs) are the highest column density (N(H I) $\geq 2 \times 10^{20}$ atoms cm^{-2}) absorbers identified in QSO spectra and the major contributors to the census of neutral gas available for star formation. DLAs are therefore widely believed to be the absorption signatures of galaxies in early stages of evolution; the study of their associated metal lines has provided us with the first accurate measurements of the abundances of a wide variety of chemical elements at high z (Lu et al. 1996; Prochaska & Wolfe 1999). Indeed, measuring the abundances in the ISM of DLAs not only gives a direct view of the evolving chemistry of galaxies over time, but is also a valuable testbed for supernova models and their theoretical yields (e.g. Pettini et al. 2000).

However, the exact nature of DLAs is still a contentious issue. Results from early DLA surveys (e.g. Wolfe et al. 1986; Lanzetta et al. 1991) led to the proposal that these systems trace the progenitors of present day spirals. More recently, Prochaska & Wolfe (1997; 1998) have argued

that this hypothesis is further supported by the kinematics of the metal absorption lines which they can best explain with large rotating disks with velocities $v_{\rm rot} \lesssim 200$ km s^{-1} (although see Ledoux et al. 1998). On the other hand, the presence of such massive disks at $z \sim 3$ is in stark contrast with the predictions of hierarchical CDM models (e.g. Kauffmann 1996) where galaxies at high redshifts are relatively compact and underluminous. In such models, the kinematics of merging proto-galactic clumps can also reproduce the shapes of the absorption lines (Haehnelt, Steinmetz, & Rauch 1998; McDonald & Miralda-Escudé 1999; Gardner et al. 2000). From the point of view of their chemical enrichment, it was shown by Pettini et al. (1997) that the distribution of DLA metallicities is displaced to lower values relative to those those of the thin and thick disk stellar populations of the Milky Way (see also Wolfe & Prochaska 1998).

At intermediate redshifts the picture is a little clearer. Direct imaging with *HST* of galaxies associated with DLAs at $z \lesssim 1$ has revealed a range of morphologies with only a minority of spirals (Le Brun et al. 1997; Rao & Turnshek 1998; Pettini et al. 2000). However, there are still concerns regarding sample bias. An absorption system at $z \lesssim 1.5$ can only be recognised as a DLA with *HST* ultraviolet spectroscopy (or 21 cm absorption, but such systems are rare). Thus QSOs behind metal- and presumably dust-rich DLAs may well be under-represented in existing surveys, given the bright magnitude limit for spectroscopy imposed by the relatively small aperture of *HST*. Since B-band luminosity and metallicity are related (e.g. Kobulnicky & Zaritsky 1999), *HST*-selected DLAs are likely to be biased in favour of absorbers of low luminosity and metallicity.

In order to make further progress on these issues, it is necessary to bring together all the information provided by deep imaging, kinematics, and chemical abundance studies into one coherent picture. In this paper we explore this approach for a high redshift DLA in the direction of the QSO Q0201+1120 which we have targeted with a number of different observations.

The compact, flat spectrum, radio source PKS 0201+113 with a faint ($R = 19.5$) optical counterpart (Condon, Hicks, & Jauncey 1977) was identified as a $z_{\rm em} = 3.61$ QSO by White, Kinney, & Becker (1993) who also reported the presence of a strong DLA at $z_{\rm abs} = 3.3875$ with an estimated N(H I) $= 2.5 \times 10^{21}$ cm^{-2}. This value of the neutral hydrogen column density is sufficiently high to produce absorption in the redshifted 21 cm line against the background radio source (de Bruyn, O'Dea, & Baum 1996; Briggs, Brinks, & Wolfe 1997), although there is still some uncertainty about the reality of these weak detections (Kanekar & Chengalur 1997). Here we present deep imaging, both from the ground and with *HST*, of the field of Q0201+1120 aimed at detecting the galaxy responsible for the DLA. In addition, we have obtained intermediate and low resolution spectroscopy of the QSO and of a number of faint sources in its proximity revealed by our images. High resolution spectroscopy of the DLA is used to study its chemical composition and velocity structure. All these data are scrutinised for clues to the nature of the object producing the damped Lyman α system.

Unless otherwise stated, we use a $\Omega_M = 0.3$, $\Omega_\Lambda = 0.7$ cosmology; h is the Hubble constant in units of 100 km s^{-1} Mpc^{-1}; and all redshifts reported in this paper are vacuum heliocentric.

2. OBSERVATIONS

Table 1 gives relevant details of the observations which we now briefly discuss.

The top panel of Figure 1 shows a new spectrum of Q0201+1120 covering the wavelength range 3500–8000 Å, obtained with the Kast double spectrograph of the Shane 3.0 m telescope at Lick Observatory. The spectral resolution is ~ 4.5 Å, a factor of ~ 2 better than the discovery spectrum by White et al. (1993). We confirm both the redshift of the QSO (within the errors of measurement) and the presence of a strong damped Lyman α line near 5330 Å; we defer precise measurements of the absorption redshift and neutral hydrogen column density to §2.3.1 and 3.1 respectively, where we present the analysis of much higher resolution echelle observations.

2.1. Imaging

The field of Q0201+1120 was imaged with the COSMIC camera (Kells et al. 1998) at the prime focus of the Palomar 5 m Hale telescope in the U_n, G, $\mathcal{R}$ photometric system designed by Steidel & Hamilton (1993) to detect primarily galaxies with redshifts in the interval $2.7 \leq z \leq 3.4$. The thinned, AR-coated Tektronix 2048×2048 CCD covers a 9.7×9.7 arcmin field sampled with a scale of 0.283 arcsec per pixel. The seeing measured from the stacked images was $\sim 0.7 - 0.9$ arcsec FWHM, and the 1σ surface brightness limits are ~ 28.56, 28.73, and 27.95 (AB) mag arcsec^{-2} in U_n, G, $\mathcal{R}$ respectively. However, the non-negligible foreground extinction in this direction ($\mathrm{E}(B-V) = 0.147$; Schlegel, Finkbeiner, & Davis 1998) makes this field less deep than most of the others observed in our Lyman break survey. Figure 2 shows contour plots of the central 30 arcsec of the $\mathcal{R}$ image before (left) and after (right) subtraction of the QSO image (achieved by appropriate scaling of the point spread function (PSF) determined from nearby stars).

We also acquired an image of this field with the Wide Field Planetary Camera (WFPC2) on *HST* through the F606W filter. To produce the final image shown in Figure 3 we combined ten individual CCD frames by 'drizzling' onto a master output pixel grid; the subtraction of the QSO used a careful modelling of the PSF appropriate for the color of the QSO and its position on the chip. Further details of the data reduction procedure can be found in Pettini et al. (2000).

A number of faint sources are present near the QSO. The objects of interest are labeled in Figures 2 and 3 and their relevant parameters are collected in Table 2; the photometry includes corrections for foreground reddening. Galaxies G1 and G3 are unlikely to be associated with the damped Lyman α system since they are both detected in U_n. The colours of G1 are consistent with those of an early-type galaxy at $z \approx 0.5$, while G3 is nearly flat-spectrum and is therefore likely to be at $z > 1$. (Note that this galaxy is very faint ($\mathcal{R} = 26.3$) so that it can barely be seen

in Figure 3 and is below the lowest contour in Figure 2). Galaxies G2 and oM6, on the other hand, are both U_n-drops and in principle could be at the redshifts of either the QSO or the DLA. A possible caveat to these conclusions is that the ground-based photometry of G1 and especially G2 is made somewhat uncertain by blending with each other and with the QSO. However, the WFPC2 F606W magnitudes of all the objects of interest here are consistent with the $\mathcal{R}$ and $(G-\mathcal{R})$ ground-based measurements in Table 2. Finally, note that the source oM6, which appears elongated in Figure 2, is clearly resolved by *HST* into two components, separated by 1.23 arcsec.

2.2. Low resolution spectroscopy

We obtained spectroscopic observations of Lyman break galaxy (LBG) candidates in the field of Q0201+1120 with the Low Resolution Imaging Spectrograph (LRIS—Oke et al. 1995) on the Keck I telescope, using different slit masks each covering approximately 4×7 arcmin. Exposure times were 2.5–3 hours per mask in separate 1800 s integrations; with the 300 grooves mm^{-1} grating the resolution of the spectra is ~ 12.5 Å. These observations resulted in 27 spectroscopically confirmed LBGs with secure redshifts. The object oM6 was among those observed; its spectrum, reproduced in the lower panel of Figure 1, exhibits a prominent Lyman α emission line at $z_{\rm em} = 3.645$. In some of the exposures the two components of oM6 are partially resolved, showing that the Lyman α emission line is stronger in the western component of the pair in Figure 3.

The emission line appears to be spectrally resolved; its profile is symmetric with FWHM ≈ 450 km s^{-1} after correction for the instrumental resolution. We measure a line flux $f_{Ly\alpha} = (8.7 \pm 0.3) \times 10^{-17}$ erg s^{-1} cm^{-2} which corresponds to a Lyman α luminosity $L_{Ly\alpha} \simeq 5.2 \times 10^{42} h^{-2}$ erg s^{-1} in our cosmology. The difference in redshift between oM6 and Q0201+1120 is only +465 km s^{-1}, well within the uncertainties (both systematic and random) in the determination of the QSO systemic redshift from the broad emission lines. We conclude that the object oM6 is *not* the DLA absorber, but it is associated with the QSO, from which it is separated by only $\sim 19 h^{-1}$ kpc.

There are several other known examples of such QSO companions; the properties of oM6 are similar, for instance, to those of the Lyman α emitter at $z = 4.695$ near the QSO BR 1202−0725 discussed by Hu, McMahon, & Egami (1996). What is particularly interesting, in the case of oM6, is the clear detection of a stellar continuum (see Figure 1). In at least this case, the companion appears to be a galaxy, possibly in the process of merging with the QSO host (Cen 2000), rather than simply a gas cloud lit up in Lyman α by its proximity to the QSO. At $z \simeq 3$ our $\mathcal{R}$ filter samples the rest-frame far-UV spectrum produced by the integrated population of O and B stars and thus provides a measure of the star-formation rate. With the transformation discussed by Pettini et al. (1998), $\mathcal{R} = 23.97$ corresponds to SFR $\simeq 12 h^{-2}\, M_\odot$ yr^{-1} in our cosmology. Correcting for dust reddening of the UV continuum as described in Adelberger & Steidel (2000), we find that $(G-\mathcal{R}) = 1.34$ implies $E(B-V) = 0.079$ and an extinction at 1500 Å $A_{1500} = 0.9$ mag. Thus, the dust corrected SFR is $\simeq 28 h^{-2}\, M_\odot$ yr^{-1}. For comparison, assuming

case B recombination and Kennicutt's (1983) calibration, $L_{Ly\alpha} \simeq 5.2 \times 10^{42} h^{-2}$ erg s^{-1} would imply only SFR $\simeq 5h^{-2}\,M_\odot$ yr^{-1}—even if the Lyman α emission line were produced entirely by stellar photoionization, which seems unlikely in this instance given the QSO proximity. Evidently, there is significant suppression of Lyman α photons within the stellar H II regions of oM6, as is normally the case in star-forming galaxies at high and low redshifts, or most of the Lyman continuum photons escape the nebula.

Returning to Figure 1, it can also be seen that, although the signal-to-noise ratio is not high, there appears to be a strong absorption feature near 5300 Å which we tentatively identify as a damped Lyman α line at $z_{\rm abs} = 3.364$ with N(H I)$= 4 \times 10^{20}$ cm^{-2} (see inset). The difference in redshift from the $z_{\rm abs} = 3.3875$ DLA in the spectrum of the QSO, corresponding to $\Delta v \simeq -1600$ km s^{-1}, is far too high for this to be the same absorbing galaxy covering both sight-lines and we must therefore be dealing with two separate absorbers. Furthermore, two out of the other 26 LBGs with spectroscopic redshifts in this field were found to be at similar redshift as the two DLAs. They are c10 and oMD26 at $z = 3.366$ and 3.368 respectively; their spectra are shown in Figure 4 and relevant properties are listed in Table 2. Thus we have found four objects at $z \simeq 3.37$ in this field, two detected in their stellar continua as Lyman break galaxies and the other two identified via absorption lines in the spectra of higher redshift sources.

Unfortunately our LRIS spectroscopy did not include object G2; in any case it would be very difficult to separate it from the QSO which is only 2.9 arcsec away and 6 magnitudes brighter. If this is the DLA, then its impact parameter from the QSO sight-line is $15h^{-1}$ kpc (proper distance). Our estimated $\mathcal{R} \simeq 25.3$ would imply that this galaxy has a rest-frame UV luminosity of about $0.7L^*$, adopting $\mathcal{R} = 24.54 = L^*$ at $z \simeq 3$ from the LBG luminosity function derived by Adelberger & Steidel (2000) for our cosmology, and making the appropriate luminosity-distance and k-corrections. If this galaxy turns out not to be at the redshift of the DLA, then the absorber must be fainter than $\mathcal{R} \approx 26.0$, or $\approx 0.4L^*$ (with the usual caveats that we would miss brighter objects if located *directly* underneath the QSO image, or if they are extended and of low surface brightness).

The remaining 24 LBGs are at redshifts between 2.167 and 3.802 and include a galaxy, m32, at $z = 3.645$ the same redshift (within the errors) as Q0201+1120 and oM6. Its spectrum is also shown in Figure 4; its projected separation of 134 arcsec from the QSO sightline (Table 2) corresponds to a comoving distance of $3.14h^{-1}$ Mpc.

Summarizing the results of this section, our deep Palomar and *HST* imaging data have shown that the strong DLA at $z_{\rm abs} = 3.3875$ in front of Q0201+1120 is part of a concentration of galaxies which includes at least four objects distributed over linear comoving dimensions of more than $5h^{-1}$ Mpc. The absorber is either a $\approx 0.7L^*$ galaxy at an impact parameter of $15h^{-1}$ kpc or is likely to be fainter than about $0.4L^*$. We have also identified two galaxies which are at the same redshift as the QSO; one of them is at a projected separation of only $19h^{-1}$ kpc from the QSO.

2.3. High Resolution Spectroscopy

In order to study in more detail the physical properties of the gas giving rise to the DLA system in Q0201+1120, we used HIRES, the echelle spectrograph on the Keck I telescope (Vogt 1992), to record the spectrum of the QSO between 4500 and 6900 Å. With the 0.86″ entrance slit the spectral resolution was 6 km s^{-1} FWHM. The observations extended over two nights; the total integration time was 40 500 s, typically made up of 4500 s long individual exposures.

The data were reduced using Tom Barlow's HIRES reduction package MAKEE[3]. Having bias subtracted and flat-fielded the individual CCD frames, MAKEE performs an optimally weighted extraction followed by wavelength calibration (on a vacuum heliocentric scale) using reference spectra of a Th-Ar hollow cathode lamp. Before joining the echelle orders, the summed data array was mapped onto a linear wavelength grid (0.03 Å pixel^{-1}); the resultant one-dimensional spectrum was then normalised to the QSO continuum determined by fitting splines to regions free of absorption lines. The signal-to-noise ratio measured in the continuum is S/N $\simeq$ 10–20; with $R = 19.5$, Q0201+1120 is at the limit of the HIRES capability. The spectrum extends from 1026 to 1573 Å in the rest frame of the $z_{\rm abs} = 3.3875$ DLA.

2.3.1. The redshift of the DLA

Figure 5 is a montage of selected metal absorption lines in the DLA. The high resolution of the echelle data reveal a complex absorption system with many individual components spread over a velocity interval of $\sim$ 270 km s^{-1}. The two components with the largest optical depths are centered at redshifts $z_{\rm abs} = 3.38632$ and 3.38684; in the strongest transitions (O I λ1302 and C II λ1334) they form a black absorption feature centered at $z_{\rm abs} = 3.38639$ which we take as the reference redshift for the DLA.

None of these redshift values agree with those reported for 21 cm absorption against the background continuum source. Three groups have searched for the 21 cm line in this damped system, with conflicting results. de Bruyn et al. (1996) using the Westerbork synthesis radio telescope found an absorption line at $z_{21} = 3.38699 \pm 0.00003$ with optical depth $\tau_{21} = 0.085 \pm 0.02$ and FWHM $= 9 \pm 2$ km s^{-1}. A detection was also reported by Briggs, Brinks, & Wolfe (1997) using the Arecibo telescope, but the feature in their spectrum had significantly different parameters: $z_{21} = 3.38716 \pm 0.00007$, $\tau_{21} = 0.037 \pm 0.008$ and FWHM $= 23 \pm 5$ km s^{-1}. Finally, Kanekar & Chengalur (1997) could see no absorption at all in data obtained with the Ooty radio telescope and of comparable sensitivity to those of the other two studies.

Here we note that the two values of z_{21} above correspond to velocities of +41 and +53 km s^{-1} relative to $z_{\rm abs} = 3.38639$ we have adopted as the zero point for the metal absorption lines.

[3]MAKEE is available from http://www2.keck.hawaii.edu:3636/realpublic/inst/hires/makeewww

Referring to Figure 5, it can be seen that these velocities fall on the red edge of the main group of absorption components, where the optical depth in the metal lines is not high. It seems unlikely that there should be such a large displacement between the optical depth of H I and those of all the other metal absorption lines (including neutral species such as O I and N I) which, as can be seen from Figure 5, agree so precisely in velocity among themselves. (Note that the damped Lyman α line itself is too broad to constrain the absorption redshift of H I within useful limits). First, the redshift differences between radio and optical data are far greater than the systematic uncertainties affecting the wavelength scale of either set of observations. Second, in two other high-z DLAs, toward the radio QSOs Q0454−020 and Q1331+170, the centroids of the 21 cm and metal absorption lines differ by less than 10 km s^{-1} (Prochaska 1999; Prochaska & Wolfe 1999). While such velocity differences may reflect geometric differences in the sight-lines probed by the radio and optical observations—and may therefore offer the means to probe the physical structure of the absorbers on small scales—the 40–50 km s^{-1} displacement found in Q0201+1120 is surprisingly large, particularly given the compact nature of the radio source. Thus, it seems to us that the redshift mismatch we have uncovered adds to the existing doubts as to the reality of the radio detections; clearly deeper 21 cm searches would be highly desirable. For the moment, it would appear that a rather high lower limit, $T_s \gtrsim 4000$ K, applies to the spin temperature of the H I gas (obtained by scaling the Kanekar & Chengalur (1997) limit to the revised value of N(H I) we deduce at §3.1 below).

We have examined the profiles of the metal absorption lines in Figure 5 for clues as to the nature of the absorber. Qualitatively, we do not see clear signs of the 'edge leading asymmetry' pattern which, according to Prochaska & Wolfe (1997), is best explained by a sight-line through a thick rotating disk. Rather, the kinematics of the gas in this DLA appear to us to be more chaotic, with components of varying strengths distributed over a larger velocity interval than the likely projected rotational speed of a $\approx L^*$ galaxy. The imaging data do not help in this respect. Galaxy G2, if it is the absorber, is very faint; our observations presumably only pick out the central, high surface brightness, region and do not allow us to make meaningful statements as to the overall morphology of this object.

3. ELEMENT ABUNDANCES

In the next stage of the analysis we deduce ion column densities by fitting the profiles of the absorption lines; this information is then used to estimate the abundances of several elements in the $z_{\rm abs} = 3.38639$ DLA.

3.1. Neutral hydrogen column density

Figure 6 shows the profile fit to the damped Lyman α line. The Lyman α forest is very crowded at these redshifts leaving only relatively few 'continuum' windows; consequently the fit is not as well constrained as is the case for DLAs in lower redshift QSOs. Our best estimate is $N(\mathrm{H\ I}) = (1.8 \pm 0.3) \times 10^{21}$ cm^{-2}. Not surprisingly, this value is lower than $N(\mathrm{H\ I}) = 2.5 \times 10^{21}$ cm^{-2} deduced by White, Kinney, & Becker (1993) from consideration of the line width in their ~ 10 Å resolution spectrum; at these high redshifts blending with Lyman α forest lines tends to boost the apparent width of a damped line with the result that the neutral hydrogen column density is easily overestimated.

3.2. Metal lines

Although our HIRES spectrum covers the wavelength region 1026 to 1573 Å in the rest frame of the DLA, many of the transitions of interest are blended with Lyman α forest lines. We have fitted all the unblended lines (or unblended portions of lines) with Voigt profiles using the VPFIT package[4]. VPFIT determines the Doppler width (b), column density (N) and redshift (z) of individual absorption components by minimizing the difference between observed and computed profiles; the number of components is kept at the minimum required by the S/N of the data.

Oscillator strengths for the transitions considered are from the compilation by Morton (1991) with subsequent revisions as summarised by Tripp, Lu, & Savage (1996). For Ni II λ1370.1 and λ1454.8 we have used the recent astrophysical and laboratory determinations by Zsargó & Federman (1998) and Fedchak & Lawler (1999). However, the f-value for one of the Ni II lines in our spectrum, λ1317.2, is not among those included in these recent studies. By fitting simultaneously all three Ni II lines in our data with $f(1317.2)$ as the free parameter, we deduced $f(1317.2) = 0.07$, approximately a factor of two lower than the theoretical value listed in Morton's (1991) compilation. This correction is similar to those which Fedchack & Lawler (1999) measured for other Ni II transitions, although data of higher S/N than those considered here are clearly required to refine this astrophysical determination.

From Figure 5 it can be seen that, as well as blending, line saturation limits the number of ion species for which reliable values of the column density can be determined. Specifically, O I λ1302.2 and C II λ1334.5 are too strong throughout to be useful for abundance studies. In the case of Si II, only λ1304.4 is sufficiently weak over part of the velocity range for VPFIT to provide a reliable solution, but the components in question—between 100 and 240 km s^{-1}—do not constitute the bulk of the absorbing gas. This leaves only N I, S II, Fe II, and Ni II as relatively unblended and unsaturated. We found that all the absorption lines of these elements (N I λ1200.0

[4]VPFIT is available at http://www.ast.cam.ac.uk/r̃fc/vpfit.html

and λ1134.7 triplets; S II λ1253.8; Fe II λ1122.0 and λ1142.4; and Ni II λ1454.8, λ1370.1, and λ1317.2) could be fitted satisfactorily with the same set of VPFIT values (b and z), leaving only the column density N to vary between the different species. The results are listed in column 2 of Table 3; typical errors returned by the fitting procedure are $\pm$15%.

The fact that for some absorption lines the velocity range 100–240 km s^{-1} is not covered (see Figure 5) is not a major concern because the column density in this group of components is less than 5% of the total. As for N I, although the main components are saturated, we found that the model parameters determined from the weaker unsaturated lines of S II, Fe II and Ni II provided the best fit to N I as well. The important point, for the discussion below, is that *it is not possible to fit the N I lines with significantly lower values of column density than that listed in Table 3.* Larger values are of course possible if the saturated N I lines hide extremely narrow components ($b < 2$ km s^{-1}) which are not present in the absorption lines from the first ions— an unlikely, but not impossible, scenario.

The species observed are the major ionization stages in H I regions, so that their ratios relative to hydrogen are a direct measure of the corresponding element abundances (column 3 of Table 3). The contributions from higher ions, which are generally small in DLAs (Viegas 1995; Howk & Sembach 1999), are likely to be even less important in this case given that: (a) the column density of neutral gas is high, and (b) the DLA is at a redshift where the intergalactic radiation field produced by QSOs is below its peak value at $z \sim 2.5$ (e.g. Madau 2000). Comparison with the solar meteoritic abundance scale of Grevesse & Sauval (1998) finally gives the relative abundances listed in the last column of Table 3. Clearly, the gas producing the $z_{\rm abs} = 3.38639$ DLA is generally metal-poor, with element abundances $Z \lesssim 1/20 Z_{\odot}$. This value is at the upper end of the range measured in DLAs at $z > 3$ (Prochaska & Wolfe 2000), but somewhat lower than the values which seem to be typical of luminous Lyman break galaxies at these redshifts (Pettini 2000 and references therein; Teplitz et al. 2000).

4. DISCUSSION OF ELEMENT RATIOS

In this section we analyse the relative abundances of the elements observed for clues to the star-formation episodes which enriched the DLA prior to $z \sim 3.4$. We follow the general approach outlined by Pettini et al. (2000) and refer the interested reader to that work for a more detailed discussion of the underlying ideas. The basic premise is that the elements in question have different nucleosynthetic histories so that their relative abundances are not expected to remain constant following a burst of star formation. Rather, the element ratios will change as stars of different masses (and therefore lifetimes) evolve off the main sequence and contribute to the chemical enrichment of the gas. As we shall see, ours is a rather ambitious goal given the uncertainties in the nucleosynthetic processes involved, in the stellar lifetimes, and in our own abundance measurements for this DLA; consequently, we can at most hope for clues, rather than definite conclusions.

4.1. Overabundance of the α-elements

One of the cornerstones of galactic chemical evolution models is the overabundance of the α-elements relative to Fe seen in Galactic metal-poor stars (where Fe is taken as the measure of metallicity). This effect is generally interpreted as reflecting the delayed production of $\approx 2/3$ of the iron by Type Ia supernovae, but in recent years this simple scenario has begun to show its limitations. First, there appear to be real differences between different elements within the α-capture group (e.g. Chen et al. 2000; Prochaska et al. 2000). The most obvious of these is the finding that the ratio [O/Fe] shows a steady increases with decreasing [Fe/H] and reaches [O/Fe] $\sim +1.0$ at [Fe/H] ~ -3. In contrast, most (but not all? — see below) of the other α-elements seem to have a constant [α/Fe] $\sim +0.5$ between [Fe/H] ~ -1 and -3 (Takeda et al. 2000 and references therein). Second, as the progenitors of Type Ia supernovae have yet to be positively identified, the timescale for the release of Fe is uncertain (see, for example, the comprehensive review by Nomoto et al. 1999). It is customary to assume a ~ 1 Gyr delay between the production of O and other α-elements in Type II SN on the one hand, and the release of the bulk of the Fe-peak elements by Type Ia SN on the other, but it is possible that the latter follow the former on much shorter intervals. For example, Regős et al. (2000) have recently pointed out that the peak in the rate of Type Ia SN formed by the edge-lit detonation of CO white dwarfs is reached less than 200 Myr after the onset of star formation. This would drastically reduce the evolutionary timescales implied by the α-elements overabundances in halo and thick-disk stars of the Milky Way.

Returning to the $z_{\rm abs} = 3.38639$ DLA, the only α-element we cover in our spectrum is sulphur. Its behavior at low [Fe/H] is not as well documented as that of other α-elements because the sulphur abundance is determined from only one, high excitation, line in the far red (S I λ8694). The studies by Francois (1988) and most recently Takeda et al. (2000) found S to track O, while Prochaska et al. (2000) found a large scatter about [S/Fe] ≈ 0 (i.e. no enhancement of sulphur) in thick disk stars with [Fe/H] $= -0.4$ to -0.6. All these authors stress the importance of carrying out more extensive surveys of the abundance of sulphur in the future.

From the last column of Table 3 it can be seen that we find [S/Fe] $\simeq +0.16$ at [Fe/H] $= -1.41$. This represents at most a mild S overabundance, given our error of ± 0.1 in the log of the ratio of any two elements and the possibility that Fe, unlike S, may be partly depleted onto dust. For comparison, Francois (1988) finds [S/Fe] $\simeq +0.6$ in Milky Way stars with [Fe/H] $= -1.4$. In the context of the discussion above, we would conclude that there has been sufficient time, since the last episode of star formation which enriched this damped Lyman α system in metals, for Fe to build up to a near-solar value relative to S. The lack of a pronounced enhancement of the α-elements now seems common to many low-metallicity DLAs (e.g. Pettini et al. 2000; Centurión et al. 2000) and has been interpreted as evidence for generally low rates of star formation.

4.2. N/α

Nitrogen is another element at our disposal which may be used to date the chemical enrichment process. At low metallicities the main source of N is thought to be primary nucleosynthesis in intermediate mass stars ($2-5M_{\odot}$) with a time delay of 250–500 Myr relative to the near-instantaneous release of O after a burst of star formation (Henry, Edmunds, & Köppen 2000; Lattanzio et al. 2000). The [N/α] ratio in DLAs exhibits a much larger scatter than any other element ratio not involving N (Lu, Sargent, & Barlow 1998; Centurión et al. 1998), with values spanning the range between secondary and primary nitrogen production. Pettini, Lipman, & Hunstead (1995) proposed that this scatter is most naturally explained as the result of the delayed release of primary N, although there are dissenting viewpoints (Izotov & Thuan 1999).

From the last column of Table 3 it can be seen that in the $z_{\rm abs} = 3.38639$ DLA we find N to be less abundant than S by a factor of 4, that is [N/S] $= -0.6$. With the assumption that [S/O] $= 0$, this corresponds to (N/O) $= -1.51$ at (O/H) $+12 = 7.58$[5]. Referring to Figure 5 of Pettini et al. (1995), it can be seen that (N/O) $= -1.51$ is a 'high' value, in the sense that it is close to that expected following the release of primary nitrogen. It is at the upper end of the range measured in DLAs and in good agreement with the typical (N/O) in blue compact and H II galaxies with (O/H) $+12 \simeq 7.6$ (e.g. see Figure 1b of Henry et al. 2000).

In concluding this section, it would seem that, within the current understanding of their time evolution, both the [α/Fe] and the [N/α] ratios measured in this DLA point to the last major episode of metal enrichment having occurred several hundred Myr prior to the redshift at which we observe the DLA. Adopting 500 Myr as the time lag for both N and Fe production, places the last major episode of star formation in this galaxy at $z > 4.3$ ($H_0 = 65$ km s^{-1} Mpc^{-1}). This conclusion is not at odds with what we already know about star formation at high redshifts, given that there seems to be no change in the luminosity function of star forming galaxies between $z = 3$ and 4.5 (Steidel et al. 1999), and that many LBGs have stellar populations older than 500 Myr (Shapley et al., in preparation).

As emphasized above, this type of analysis is based on many assumptions whose validity remains to be verified; ultimately it will only be possible to establish whether element ratios give a self-consistent picture by conducting a full study of a large body of high quality measurements. However, we note that at least one other well-studied high-z DLA has similar chemical properties to those deduced here. From VLT/UVES observations of the $z_{\rm abs} = 3.3901$ DLA in Q0000−2620 Molaro et al. (2000) deduce [α/Fe-peak] $\simeq +0.2$ and (N/O) $= -1.69$ at (O/H) $+12 = 7.01$. So this may well be another example of a DLA galaxy with low, or episodic, star formation which started before $z = 4.3$.

[5]We apologise to the reader for this sudden change of notation, but nearly all published measurements of the N and O abundances are in these units. (N/O) and (O/H) are the logarithmic values of the element ratios by number, without reference to the solar values.

5. Summary and Conclusions

In this paper we have presented imaging and spectroscopic observations aimed primarily at investigating the nature of the absorber giving rise to the strong damped Lyman α system at $z_{\rm abs} = 3.38639$ in front of Q0201+1120. Our main findings can be summarised as follows.

1. The DLA is part of a concentration of matter which includes at least four galaxies at $z \simeq 3.37$ over transverse dimensions of at least $5h^{-1}$ Mpc (comoving). Two of the galaxies are seen directly via their UV stellar continua, while two others (including the DLA) are detected in absorption against higher redshift sources. Since we have so far obtained spectra for only about one quarter of the U-drop candidates in this field, it is likely that the structure includes other objects at $z \simeq 3.37$.

2. We have found a promising candidate for the absorber in a photometric Lyman break object only 2.9 arcsec away from the QSO sight-line. If confirmed by future spectroscopy to be at the absorption redshift, then the galaxy associated with this DLA has a UV luminosity of about $0.7L^*$ and a linear extent of at least $15h^{-1}$ kpc. Otherwise the absorber is likely to be fainter than about $0.4L^*$.

3. The H I gas producing the damped system is highly turbulent, with a spin temperature $T_s \gtrsim 4000$ K and complex absorption line profiles, consisting of many discrete components spanning ~ 270 km s^{-1}. Neither is what one may have expected from a cold, rotationally supported, disk.

4. The DLA has a metallicity $Z \simeq 1/20 Z_\odot$, at the upper end of the distribution of values of $Z_{\rm DLA}$ at these redshifts, but lower than those deduced for other luminous Lyman break galaxies, although the data here are still very sparse. Further, it exhibits no marked overabundance of the α-elements (in this case S) relative to Fe, and a relatively high (N/α) ratio for its low metallicity. Both element ratios can be understood if there has been a relatively quiescent interval, lasting more than ~ 500 Myr, since the last major burst of star formation in this galaxy, allowing the delayed release of Fe from Type Ia SN and of N from AGB stars of intermediate mass. If this reasoning is correct, the star formation episode responsible for producing the heavy elements we see occurred at $z \gtrsim 4.3$. The chemical properties of this absorber are similar to those of another high-z DLA, at $z_{\rm abs} = 3.3901$ in Q0000−2620, which has been extensively studied with both the Keck and VLT echelle spectrographs.

Firm conclusions on the nature of DLAs at high redshifts are hampered by the lack of follow-up spectroscopy of galaxy G2. If this is indeed the absorber, it would be only the second case where a high-z DLA has been identified with a Lyman break galaxy, after the $z_{\rm abs} = 3.151$ system in Q2233+1310 (Steidel, Hamilton, & Pettini 1995; Djorgowski et al. 1996), although others have been detected in Lyman α emission (e.g. Fynbo, Burud, & Møller 2000 and references

therein). In general our deep Lyman break imaging has shown that the galaxies producing DLAs at $z \gtrsim 3$ must be significantly sub-L^* in their stellar continua (e.g. Steidel et al. 1995; Steidel et al. 1998) and that detections such as this one are the exception rather than the rule.

We conclude that, although the statistics are still very limited, DLAs seem to sample a wide range of the luminosity function of galaxies at $z \simeq 3$. QSO absorption line spectroscopy still gives us the most precise measurements of many important physical properties of high redshift gas. However, only by combining it with deep imaging will it be possible to realise its full potential for unravelling the nature and evolution of galaxies at early times.

We are grateful to the staff of the Palomar and Keck Observatories for their competent technical assistance. Our collaborators in the LBG survey project, Kurt Adelberger, Mark Dickinson, Mauro Giavalisco, and Mindy Kellogg, generously helped with various aspects of the data acquisition and reduction. C.C.S. acknowledges support from the National Science Foundation through grant AST 95-96229 and from the David and Lucile Packard Foundation.

REFERENCES

Adelberger, K.L., & Steidel, C.C. 2000, ApJ, 544, in press (astro-ph/0001126)

Briggs, F.H., Brinks, E., & Wolfe, A.M. 1997, AJ, 113, 467

Cen, R. 2000, ApJ, 533, L1

Centurión, M., Bonifacio, P., Molaro, P., & Vladilo, G. 1998, ApJ, 509, 620

Centurión, M., Bonifacio, P., Molaro, P., & Vladilo, G. 2000, ApJ, 536, 540

Chen, Y.Q., Nissen,P.E., Zhao, G., Zhang, H.W., & Benoni, T. 2000, A&AS, 141, 491

Condon, J.J., Hicks, P.D., & Jauncey, D.L. 1977, AJ, 82, 692

de Bruyn, A.G., O'Dea, C.P., & Baum, S.A. 1996, A&A, 305, 450

Djorgovski, S.G., Pahre, M.A., Bechtold, J., & Elston, R. 1996, Nature, 382, 234

Fedchak, J. A., & Lawler, J. E. 1999, ApJ, 523, 734

Francois, P. 1988, A&A, 195, 226

Fynbo, J.U., Burud, I. & Møller, P. 2000, A&A, 358, 88

Gardner, J.P., Katz, N., Hernquist, L., & Weinberg, D.H. 2000, ApJ, submitted (astro-ph/9911343)

Grevesse, N., & Sauval, A.J. 1998, Space Sci Rev, 85, 161

Haehnelt, M. G., Steinmetz, M., & Rauch, M. 1998, ApJ, 495, 647

Henry, R. B. C., Edmunds, M. G., & Köppen, J. 2000, ApJ, 540, in press (astro-ph/0004299)

Howk, J.C., & Sembach, K.R. 1999, ApJ, 523, L141

Hu, E.M., McMahon, R.G., & Egami, E. 1996, ApJ, 459, L53

Kanekar, N., & Chengalur, J.N. 1997, MNRAS, 292, 831

Kauffmann, G. 1996, MNRAS, 281, 475

Kells, W., Dressler, A., Sivaramakrishnan, A., Carr, D., Koch, E., Epps, H., Hilyard, D., & Pardeilhan, G. 1998, PASP, 110, 1487

Kennicutt, R.C. 1983, ApJ, 272, 54

Kobulnicky, H.A., & Zaritsky, D. 1999, ApJ, 511, 118

Lanzetta, K. M., McMahon, R. G., Wolfe, A. M., Turnshek, D. A., Hazard, C., & Lu, L. 1991, ApJS, 77, 1

Lattanzio, J., Pettini, M., Tout, C. A., & Carigi, L. 2000, A&A, submitted

Le Brun, V., Bergeron, J., Boisse, P., & Deharveng, J. M. 1997, A&A, 321, 733

Ledoux, C., Petitjean, P., Bergeron, J., Wampler, E.J., & Srianand, R., 1998, A&A, 337, 51

Lu, L., Sargent, W. L. W., Barlow, T.A. 1998, AJ, 115, 55

Lu, L., Sargent, W. L. W., Barlow, T. A., Churchill, C. W., Vogt, S. S. 1996, ApJS, 107, 475

Madau, P. 2000, Phil. Trans. Roy. Soc. London A., in press (astro-ph/0003096)

McDonald, P., & Miralda-Escudé, J. 1999, ApJ, 519, 486

Molaro, P., Bonifacio, P., Centurión, M., D'Odorico, S., Vladilo, G., Santin, P., & Di Marcantonio, P. 2000, ApJ, in press (astro-ph/0005098)

Morton, D. 1991, ApJS, 77, 119

Nomoto, K., Umeda, H., Hachisu, I., Kato, M., Kobayashi, C., & Tsujimoto, T. 1999, in Type Ia Supernovae: Theory and Cosmology, ed. Truran, J., & Niemeyer, J. (Cambridge: University Press), in press (astro-ph/9907386)

Oke, J.B., et al. 1995, PASP, 107, 3750

Pettini, M. 2000, Philos. Trans. R. Soc. Lond. A, 358, 2035 (astro-ph/0001075)

Pettini, M., Ellison, S. L., Steidel, C. C., Shapley, A. E., & Bowen, D. V. 2000, ApJ, 532, 65

Pettini, M., Kellogg, M., Steidel, C.C., Dickinson, M., Adelberger, K.L., & Giavalisco, M. 1998, ApJ, 508, 539

Pettini, M., Lipman, K., & Hunstead, R.W. 1995, ApJ, 451, 100

Pettini, M., Smith, L.J., King, D.L., & Hunstead, R.W. 1997, ApJ, 486, 665

Prochaska, J.X. 1999, in ASP Conf. Ser. 156, Highly Redshifted Radio Lines, , ed. C. Carilli, S.J.E. Radford, K.M. Menten, & G.I. Langston (San Francisco:ASP), 140

Prochaska, J. X., Naumov, S.O., Carney, B.W., McWilliam, A., & Wolfe, A. M. 2000, ApJ, submitted

Prochaska, J. X., & Wolfe, A. M. 1997, ApJ, 487, 73

Prochaska, J. X., & Wolfe, A. M. 1998, ApJ, 507, 113

Prochaska, J.X., & Wolfe, A.M. 1999, ApJS, 121, 369

Prochaska, J. X., & Wolfe, A. M. 2000, ApJ, 533, L5

Rao, S.M., & Turnshek, D.A. 1998, ApJ, 500, 115

Regős, E., Tout, C.A., Wickramasinghe, D., Hurley, J.R., and Pols, O.R. 2000, ApJ, submitted.

Schlegel, D.J., Finkbeiner, D.P., & Davis, M. 1998 ApJ, 500, 525

Steidel, C.C., Adelberger, K.L., Dickinson, M., Giavalisco, M., Pettini, M. & Kellogg, M. 1998, ApJ, 492, 428.

Steidel, C.C., Adelberger, K.L., Giavalisco, M., Dickinson, M., & Pettini, M. 1999, ApJ, 519, 1

Steidel, C.C., & Hamilton, D. 1993, AJ, 105, 2017

Steidel, C.C., Pettini, M., & Hamilton, D. 1995, AJ, 110, 2519

Takeda, Y., Takada-Hidai, M., Sato, S., Sargent, W.L.W., Lu., L., Barlow, T.A., & Jugaku, J. 2000, ApJ, submitted (astro-ph/0007007)

Teplitz, H.I. et al. 2000, ApJ, in press (astro-ph/0005254)

Tripp, T.M., Lu, L., & Savage, B. D. 1996, ApJS, 102, 239

Viegas, S.M. 1995, MNRAS, 276, 268

Vogt, S.S., 1992, in ESO Conf. and Workshop Proc. 40, High Resolution Spectroscopy with the VLT, ed. M.H. Ulrich (Garching, ESO), 223

White, R.L., Kinney, A.L., & Becker, R.H. 1993, ApJ, 407, 456

Wolfe, A.M., & Prochaska, J.X. 1998, ApJ, 494, L15

Wolfe, A. M., Turnshek, D. A., Smith, H. E., & Cohen, R. D. 1986, ApJS, 61, 249

Zsargó, J., & Federman, S. R. 1998, ApJ, 498, 526

This preprint was prepared with the AAS LaTeX macros v4.0.

Table 1. Summary of Observations

Object/Field	Telescope	Instrument	Filter/Grating	Int Time (s)
Q0201+1120	Hale 5m	COSMIC	U_n	27 000
Q0201+1120	Hale 5m	COSMIC	G	7 200
Q0201+1120	Hale 5m	COSMIC	$\mathcal{R}$	3 600
Q0201+1120	*HST*	WFPC2	F606W	10 800
Q0201+1120	Lick 3m	Kast	600/4340 & 600/7500	14 400
Q0201+1120	Keck I 10m	HIRES		40 500
Galaxy oM6	Keck I 10m	LRIS	300/5000	10 800
Galaxy m32	Keck I 10m	LRIS	300/5000	10 800
Galaxy c10	Keck I 10m	LRIS	300/5000	10 800
Galaxy oMD26	Keck I 10m	LRIS	300/5000	10 800

Table 2. Parameters of Sources in the Field of Q0201+1120

Name	ΔRA (″)[a]	ΔDecl. (″)[a]	$\mathcal{R}$	$G-\mathcal{R}$	U_n-G	Redshift	Δr (Mpc)[b]
Q0201+1120	0.0	0.0	19.23	0.93	≥ 5.20[c]	3.638	0.0
G1	+0.9	+0.4	22.23	1.48	1.63	...	...
G2	+2.8	−0.9	25.3:[d]	0.5:[d]	> 1.7 :[d]	...	...
G3	+3.4	−2.7	26.3	0.2	0.3	...	...
oM6	+1.3	−3.5	23.97	1.34	> 2.62	3.645	0.085
m32	+113.5	+71.5	25.21	0.79	> 1.99	3.645	...
c10	−116.6	+166.1	24.07	0.70	> 2.68	3.366	4.61
oMD26	−98.0	+204.7	24.72	0.83	≥ 1.72[c]	3.368	5.15

[a]Relative to Q0201+1120.

[b]Comoving distance from Q0201+1120 sightline at $z = 3.37$ ($\Omega_M = 0.3$, $\Omega_\Lambda = 0.7$, $h = 1$).

[c]Formally detected in U_n at the 1σ level.

[d]The photometry of G2 is uncertain because of its proximity to G1 and the QSO.

Table 3. Ion Column Densities and Element Abundances in the $z_{\rm abs} = 3.38639$ DLA

X^i	log $N(X^i)$[a]	log $N(X^i)/N(\mathrm{H}^0)$	log $(X/\mathrm{H})_\odot$[b]	$[X/\mathrm{H}]$[c]
H^0	21.26	...	...	...
N^0	15.33	−5.93	−4.08	−1.85
Si^+	> 14.00[d]	...	...	...
S^+	15.21	−6.05	−4.80	−1.25
Fe^+	15.35	−5.91	−4.50	−1.41
Ni^+	13.84	−7.42	−5.75	−1.67

[a]Log of the column density of ion X^i; typical errors are ±15%.

[b]Solar meteoritic abundance scale from Grevesse & Sauval (1998).

[c]$[X/\mathrm{H}] = \log\,(X/\mathrm{H}) - \log\,(X/\mathrm{H})_\odot$.

[d]This value refers only to gas in the velocity interval 100—240 km s^{-1} (relative to $z_{\rm abs} = 3.38639$) which accounts for only a small fraction of the total column density.

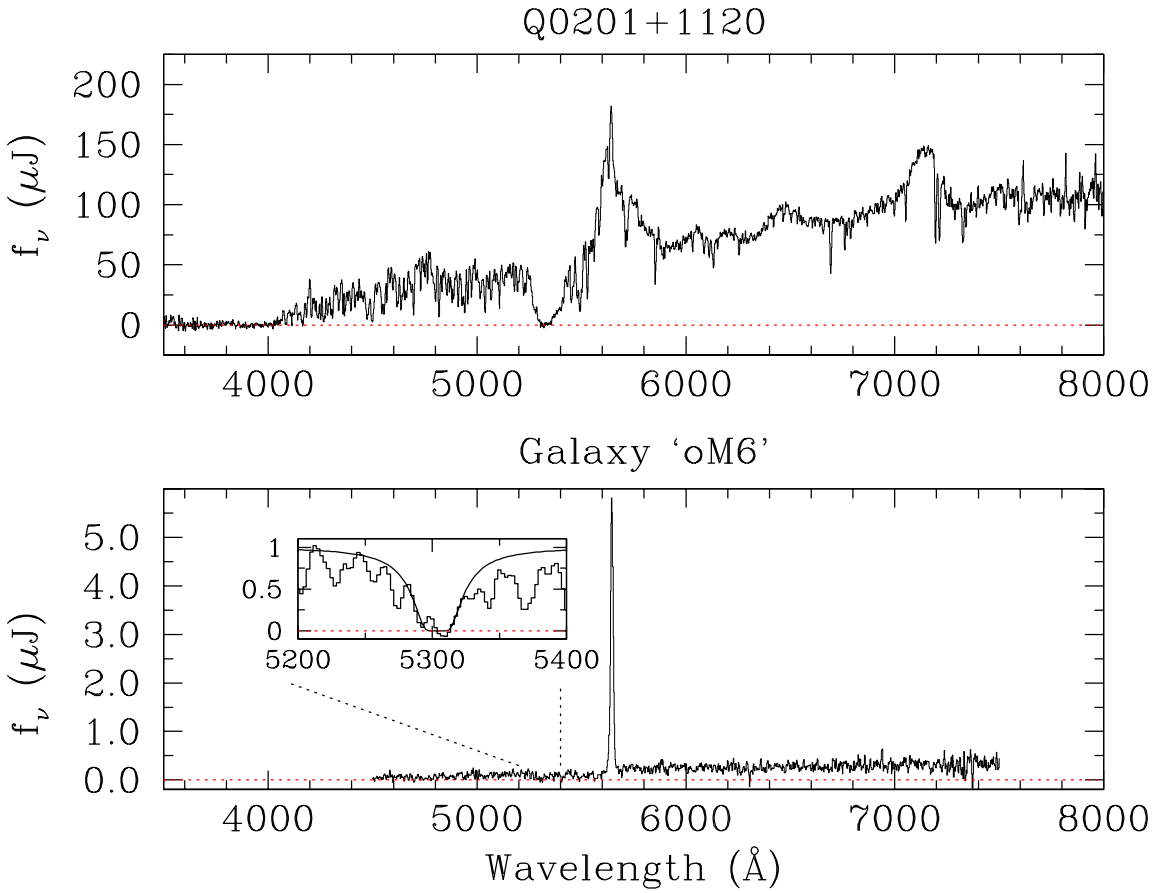

Fig. 1.— *Upper panel:* Lick spectrum of Q0201+1120; the resolution is $\sim$ 4.5 Å. *Lower panel:* LRIS spectrum of galaxy oM6; the resolution is $\sim$ 12 Å. See Table 1 for additional details of the observations. The inset shows the profile fit to the absorption feature near 5300 Å which we tentatively identify as damped Lyman α at $z_{\rm abs} = 3.364$ with N(H I)$= 4 \times 10^{20}$ cm^{-2}.

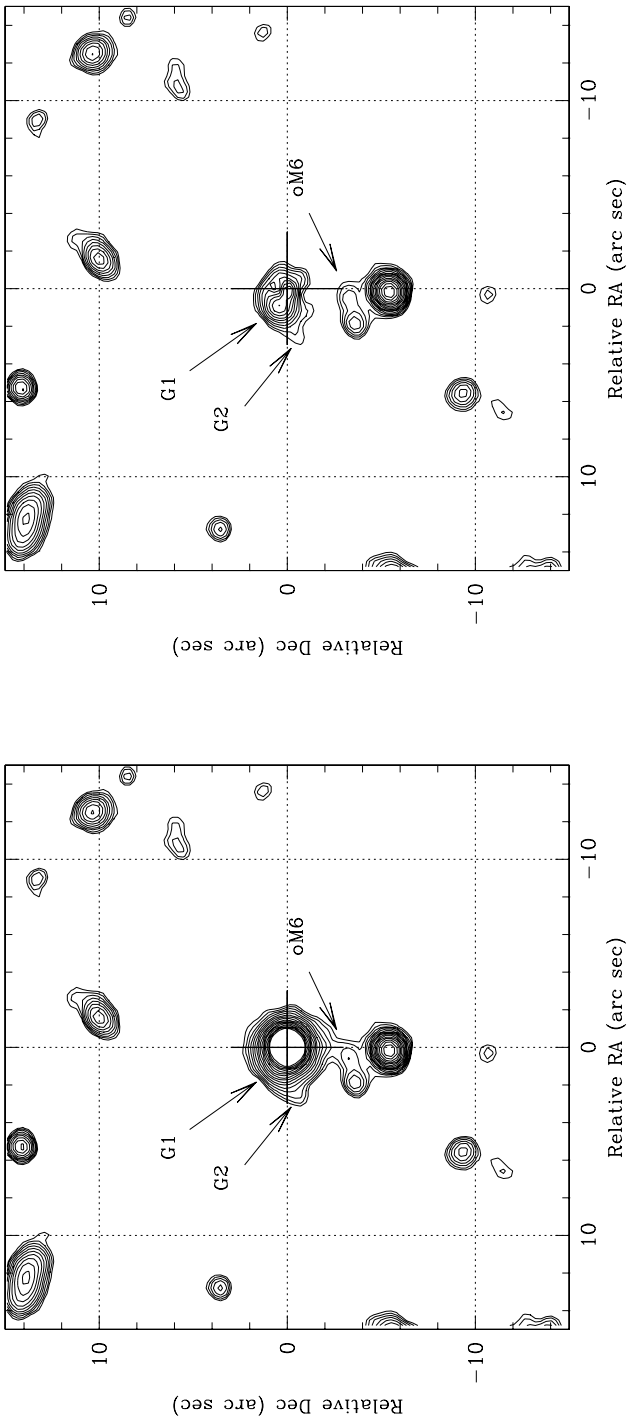

Fig. 2.— Contour plots of the central 30 arcsec of the Palomar $\mathcal{R}$-band image of the field of Q0201+1120 before (left) and after (right) subtraction of the QSO image.

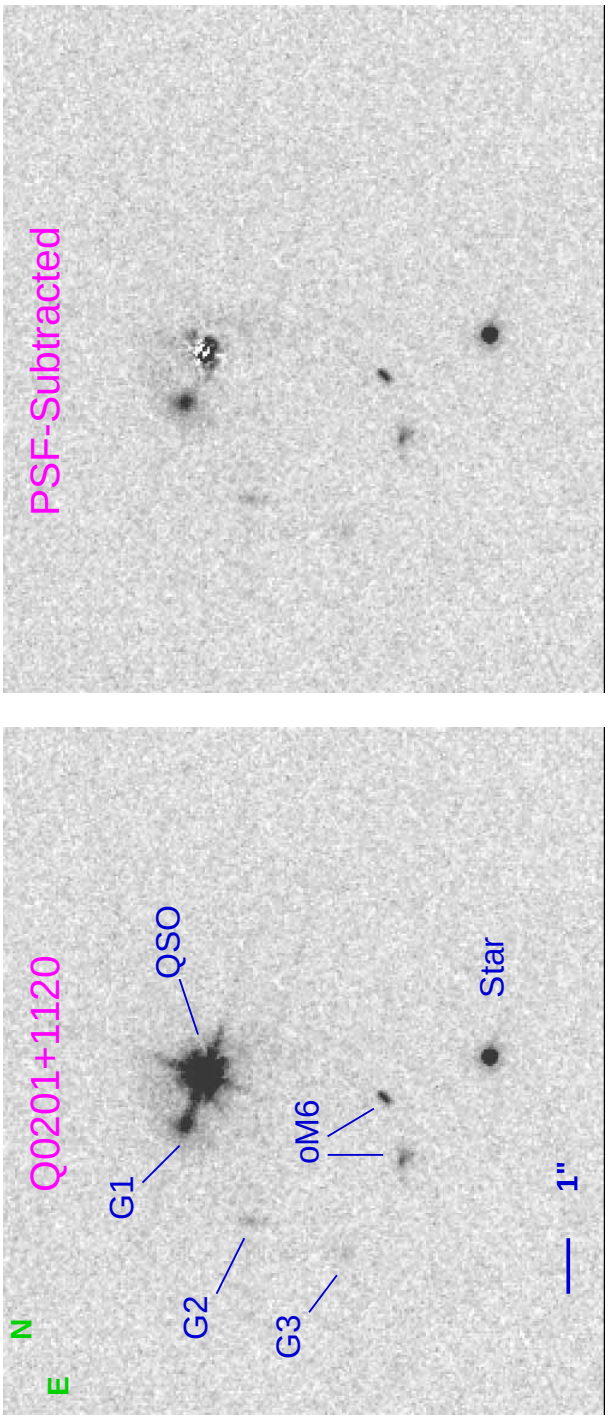

Fig. 3.— F606W WFPC2 image of the field of Q0201+1120 before (left) and after (right) subtraction of the QSO image.

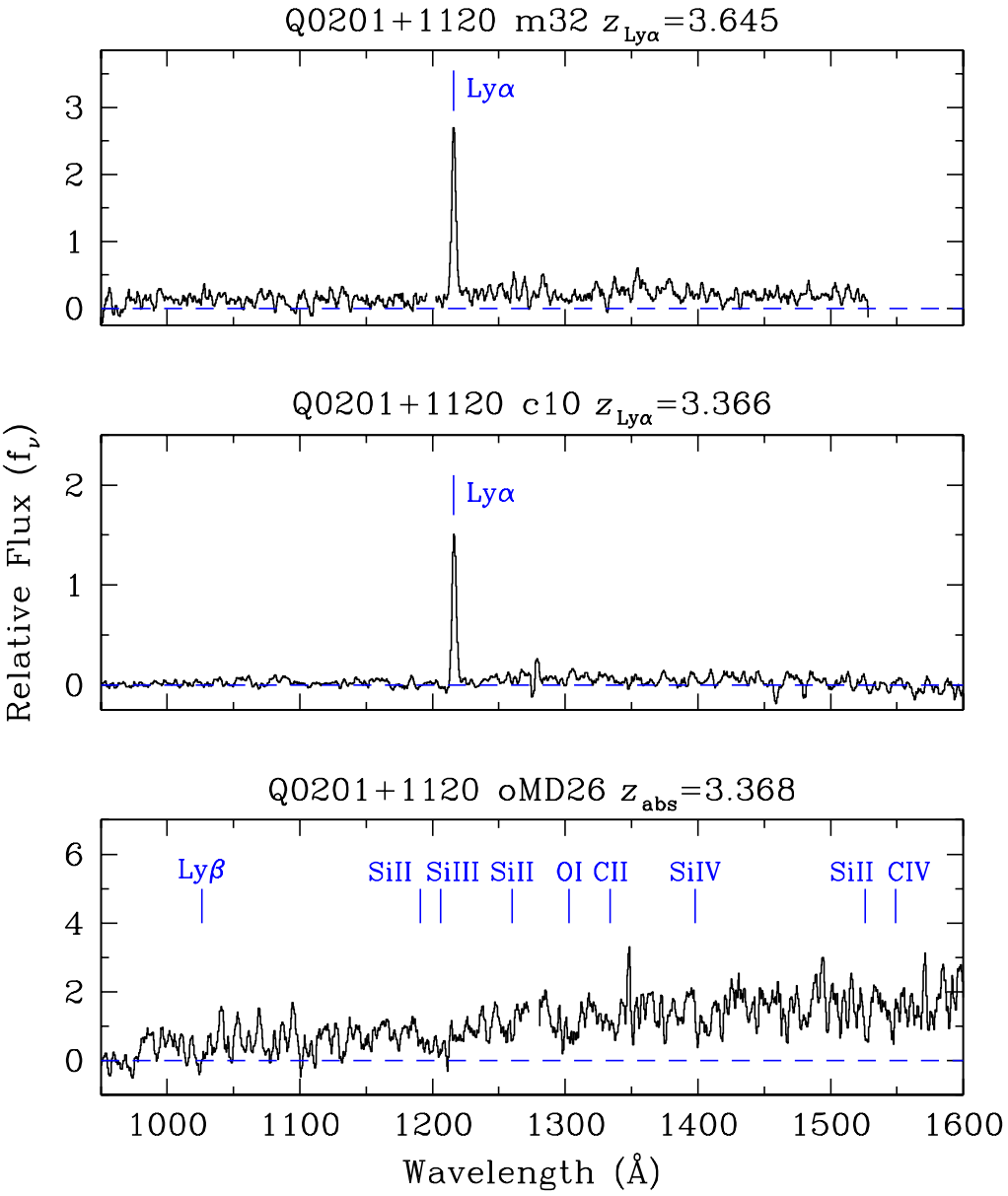

Fig. 4.— LRIS spectra of Lyman break galaxies m32, c10 and oMD26 reduced to the respective rest frames. The redshifts of m32 and c10 are determined from their prominent Lyman α emission lines; that of oMD26 is from the strongest interstellar absorption lines, as indicated. The redshift of m32 is close to those of Q0201+1120 and oM6, while c10 and oMD26 are at similar redshifts as the damped Lyman α system in Q0201+1120 (see Table 2).

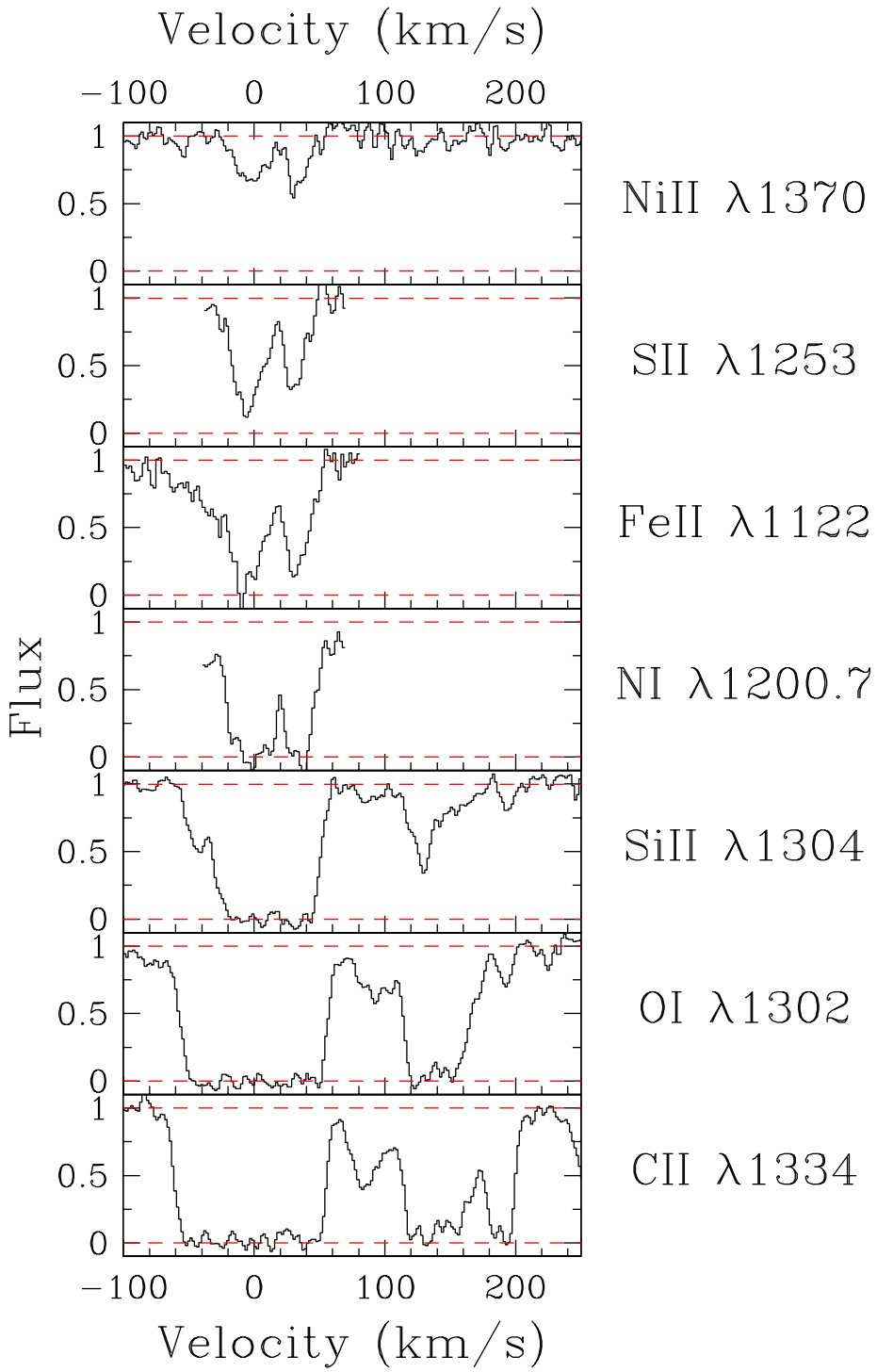

Fig. 5.— Normalized profiles of selected metal absorption lines in the damped Lyman α system at $z_{\rm abs} = 3.38639$; the velocity scale is relative to this redshift.

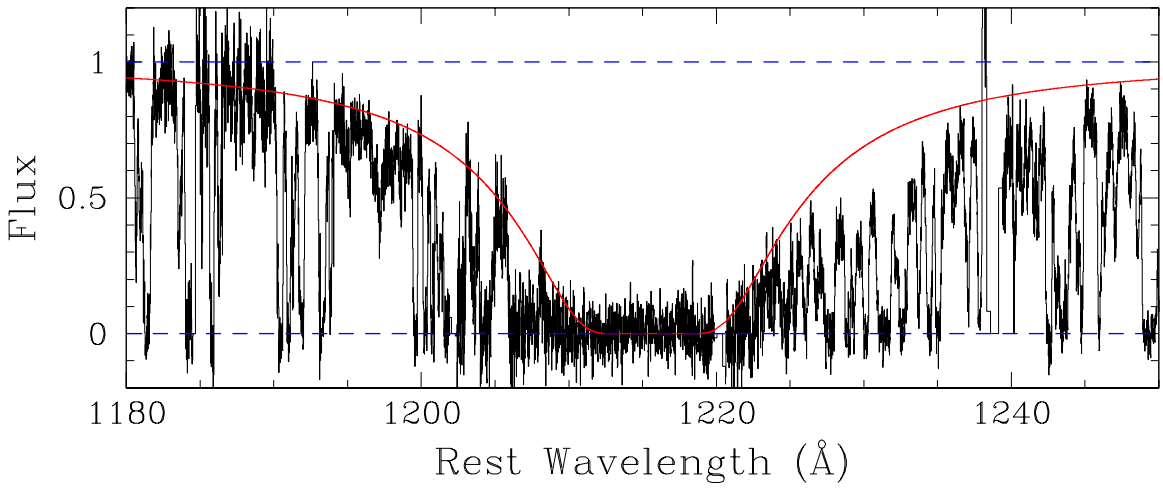

Fig. 6.— Portion of the HIRES spectrum of Q0210+1120 showing the damped Lyman α line at $z_{\rm abs} = 3.38639$. The profile fit shown is for a column density $N({\rm H\ I}) = 1.8 \times 10^{21}$ cm^{-2}.